GEOLOGICAL JOURNAL
Geol. J. **52**: 131–140 (2017)
Published online 13 November 2015 in Wiley Online Library
(wileyonlinelibrary.com). DOI: 10.1002/gj.2739

Inverted relief landforms in the Kumtagh Desert of northwestern China: a mechanism to estimate wind erosion rates

ZHEN-TING WANG[1,2]*, ZHONG-PING LAI[3] and JIAN-JUN QU[2]

[1] *State Key Laboratory of Earth Surface Processes and Resource Ecology, Beijing Normal University, Beijing, China*
[2] *Dunhuang Gobi Desert Research Station, Cold and Arid Regions Environmental and Engineering Research Institute, CAS, Dunhuang, China*
[3] *State Key Laboratory of Biogeology and Environmental Geology, China University of Geosciences, Wuhan, China*

Although commonly found in deserts, our knowledge about inverted relief landforms is very limited. The so-called 'Gravel Body' in the northern Kumtagh Desert is an example of an inverted relief landform created by the exhumation of a former fluvial gravel channel. The common occurrence of these landforms indicates that fluvial processes played an important role in shaping the Kumtagh Desert in the past 151 ka. A physical model is presented to reconstruct the palaeohydrology of these fluvial channels in terms of several measurable parameters including terrain slope, boulder size, and channel width. Combining the calculated palaeoflood depth, the maximal depth of channel bed eroded by wind, and the current height of inverted channels with the age of the aeolian sediments covered by gravels, the local wind erosion rate is estimated to be 0.21–0.28 mm/year. It is shown that wind erosion occurring in the Kumtagh Desert is no more severe than in adjacent regions. Since the modern Martian environment is very similar to that of hyperarid deserts on Earth, and Mars was once subjected to fluvial processes, this study will be helpful for understanding the origin of analogous Martian surface landforms and their causative processes.

Received 24 September 2015; accepted 9 October 2015

KEY WORDS wind erosion; inverted relief; palaeochannel; Kumtagh Desert; Martian surface

1. INTRODUCTION

Inverted relief, also known as inverted topography, inversion of relief, or topographic inversion, refers to an episode in landscape evolution when a former valley bottom becomes a topographic high ridge, bounded by areas of lower relief on each side (Pain and Ollier, 1995). This type of landform is generally constituted of, or covered by, materials resistant to wind erosion such as gravel, lava, or silcrete. Although commonly found in deserts, especially within yardang fields, the process generating inverted relief (for example, of former riverbeds and lacustrine deposits) is not well understood (Laity, 2009, 2011; Goudie, 2013). The wind erosion rate (deflation and abrasion) is of primary interest in aeolian research, and published global statistics shows that its magnitude varies from 10^{-3} to 10^{2} mm/year (Rohrmann *et al*., 2013). The study of inverted relief can be used to determine wind erosion rate in windy and arid regions.

Many examples in the review of Pain and Ollier (1995) indicate that inverted relief is widespread globally. The inverted palaeochannels in arid and semi-arid regions occur in the Western Desert of Egypt (Brookes, 2003), the Atacama Desert of South America (Morgan *et al*., 2014), the Sharqiya or Wahiba Sands of Oman (Maizels, 1987, 1990), and the Great Salt Lake Desert of North America (Oviatt *et al*., 2003). The current Martian surface is similar to that of deserts on Earth. Inverted relief is a universal feature on Mars, and some analogical studies have been conducted (Malin and Edgett, 2003; Pain *et al*., 2007; Williams, 2007; Morgan *et al*., 2014). In China, there are widespread areas of desert, Gobi (gravel desert), and yardangs (and other wind-eroded lands), comprising 6.84×10^{5}km^{2}, 5.70×10^{5}km^{2}, and 2.90×10^{4}km^{2}, respectively (Wang, 2011). To date, only limited examples of inverted relief from such a large dryland area have been systematically reported. The earliest work is from the Lop Nor depression, where silty beds were raised into a topography of ridges and hillocks after the surrounding softer sediments

*Correspondence to: Z-T. Wang, Dunhuang Gobi Desert Research Station, Cold and Arid Regions Environmental and Engineering Research Institute, CAS, Dunhuang 736200, China. E-mail: wangzht@lzu.edu.cn

were eroded by wind (Horner, 1932). The second is the well-studied 'Shell Bar' in the Qaidam Basin. This feature is composed of millions of shells and is protected from erosion by a solidified salt-shell crust layer, several decimetres thick. The Shell Bar was originally interpreted as a shoreline or lacustrine deposit and was previously dated to approximately 30–40 ka BP (Chen and Bowler, 1986; Zhang *et al*., 2008). Recently, it was re-interpreted as a remnant river channel that crossed an exposed lake bed during a regressive lake phase. The inverted channel has been dated by optically stimulated luminescence (OSL) to have formed at 100 ka (Lai *et al*., 2014). This landform indicates that the Qaidam Basin has been erosive since that time.

The methods of determining wind erosion rate are varied and operate over different timescales. A number of sand traps and saltation impact sensors (Goossens *et al*., 2000; Pelt *et al*., 2009) can be employed to collect the moving sediment in a wind erosion event lasting several hours or days. The WEQ (Woodruff and Siddoway, 1965), WEPS (Hagen, 1991), and WEAM models (Shao *et al*., 1994) are appropriate to use when the gauged data of wind speed and direction exist over seasonal or annual timescales. For the short-term (<100 years) erosion of yardangs, both field monitoring (Al-Dousari *et al*., 2009) and physical modelling (Wang *et al*., 2011) are best used. For longer timescales, the techniques of geochronology have to be utilized. Cosmic ray dating can give the exposure time of sediments if the radioactive half-life of an isotope is lengthy compared to the erosional timescale. The concentration of ^{10}Be in rocks is commonly used to reflect the long-term erosion rate (Lal, 1991; Ruszkiczay-Rudiger *et al*., 2011; Rohrmann *et al*., 2013). This method is mostly suitable for stable landforms. The age of the deposit and information detailing the removed sediment cover may also be used to estimate the wind erosion rate (Clarke *et al*., 1996; Bristow *et al*., 2009; de Silva *et al*., 2010). The latter method often generates a conservative estimate of erosion rate (Rohrmann *et al*., 2013), but it benefits from a number of well-established, accurate dating techniques, enabling Quaternary scientists to date events on timescales ranging from single to millions of years (Walker, 2005). One challenge with this method is how to reconstruct the elevation of the former terrestrial surface, as most surficial materials have been removed by wind erosion.

In this study, we firstly describe an example of inverted relief landform from the Kumtagh Desert and then develop a physical model for estimating the local wind erosion rate.

2. REGIONAL SETTING

The main body of the Kumtagh Desert has a broom-like plan view and occurs on the north bajada of the Altyn Mountains (Fig. 1). The Desert is restricted to the north by the Beishan Mountains and the Achike Valley and is adjacent to the Lop Nor depression to the northwest and the Dunhuang Oasis to

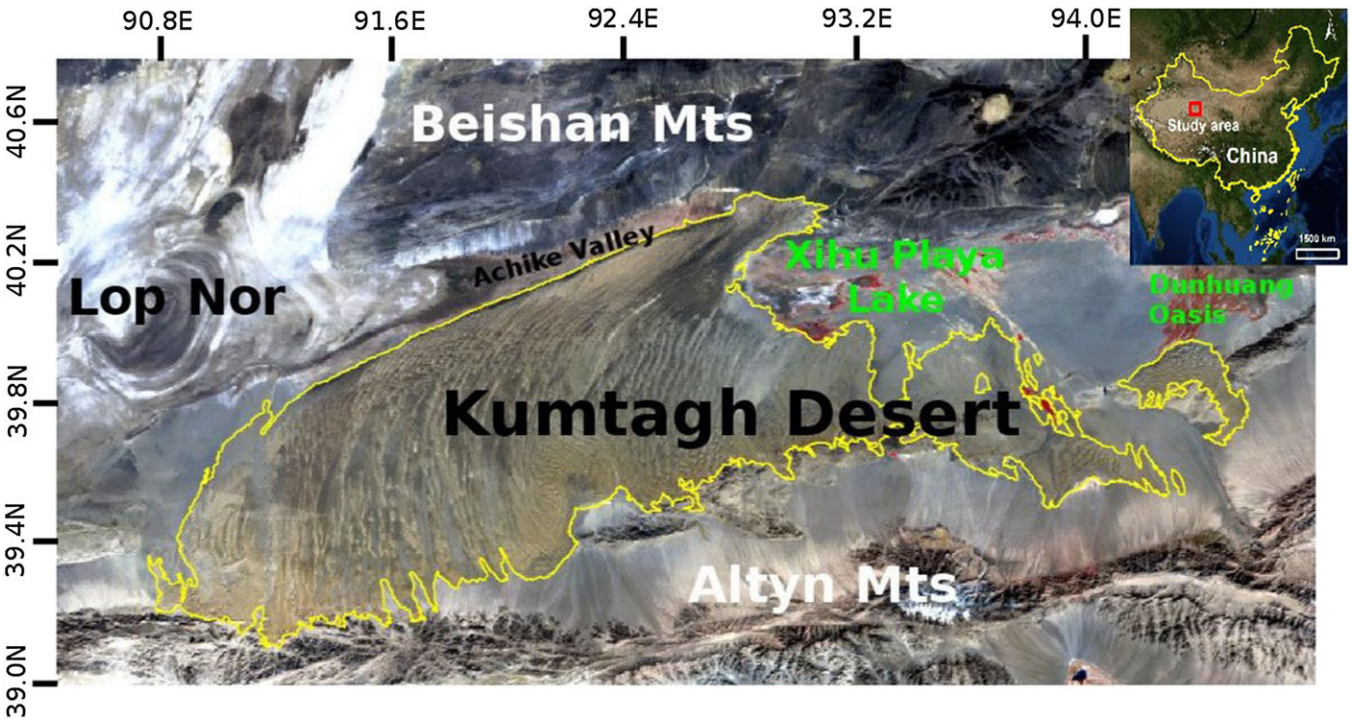

Figure 1. Map of the study area. This figure is available in colour online at wileyonlinelibrary.com/journal/gj

DOI: 10.1002/gj

the east in NW China. As the seventh largest dune field in China, it comprises a total area of approximately $2.0 \times 10^4 km^2$ (Wang, 2011). The relief varies between 800 to 2600 m above sea-level. The annual precipitation in this extremely arid desert is approximately 10 mm (Wang, 2011; Lu, 2012). The area is prone to increased precipitation events, and the annual precipitation during 2008–2013 was 83.3 mm, with the maximum average monthly precipitation of 17.2 mm occurring in July (Kang *et al*., 2015). Using the classification of Fryberger (1979), the modern wind regime in the northern part of the desert comprises an obtuse bimodal intermediate-energy wind environment (Qu *et al*., 2007). The resultant drift direction is southwestward. The annual average wind speed at a height of 10 m above the ground is 3.42 m/s (Zhang *et al*., 2010). Studies of grain-size distribution, median diameter, standard deviation, skewness, and kurtosis imply that sediment types and depositional environments are diverse (He *et al*., 2009). Both aeolian and alluvial/lacustrine sediments are commonly observed in the desert. There are two major source provenance zones revealed by mineral and geochemical composition of sediments (Xu *et al*., 2011). Sediments derived from the highlands of the Altyn Mountains are often transported by torrential floods to the depositional basin comprising the desert at lower elevations. The second source comprises alluvial/lacustrine deposits in the Achike Valley and those of the Xihu playa lake which are eroded and transported by the strong northeasterly wind into the desert basin.

Comprehensive scientific expeditions into the Desert were not conducted until 2004 because of its harsh natural environment (E *et al*., 2006; Wang *et al*., 2009). There is currently ongoing debate amongst Chinese desert geomorphologists as to the definition and classification of the Desert's feather-like dune fields (Dong *et al*., 2008; Dong, 2009; Wang *et al*., 2009; Qu *et al*., 2011; Qian *et al*., 2015). Previous geomorphological studies in the Kumtagh Desert by Chinese scientists during the last decade have been selectively translated and reviewed by Dong and Lv (2014).

3. MATERIALS AND METHODS

3.1. Inverted relief

3.1.1. Description

'Gravel bodies' are a unique landform of the Kumtagh Desert distinguished from other deserts in China (E *et al*., 2008; Lu, 2012). Five morphological types, i.e. platform, girder, replat, sheet and strip, and ring are reported (Dong and Qu, 2009; Dong *et al*., 2010; Dong *et al*., 2011). These terms provide a vivid description of this feature although the classification criterion is vague. The rarely occurring 'gravel ring' is actually identical to the 'gravel sheet and strip' type because its gravelled inner part has been buried by aeolian sand grains. Here we describe them simply as elongated and subround 'gravel bodies' in terms of their plan-view shapes. The typical morphologies are provided in Figure 2. Elongated 'gravel bodies' are 10–200 m long, 1–10 m wide, and 2–15 m high. Most of them are relatively straight, less than 30 m in length, with a widespread distribution. Some longer ones extend into the neighbouring linear dunes. Subround 'gravel bodies' are 2–30 m high, 5–50 m in diameter, with flat or sharp top surfaces. They often stand alone in inter-dune corridors where zibars composed of coarse sediments are developing. A few subround 'gravel bodies' have collapsed, scattering their gravel irregularly.

3.1.2. Interpretation

The feature in Figure 2 should not be confused with yardangs which refer to erosional ridges formed in slightly compacted, fine-grained, cohesive sediments. Mature yardangs are generally streamlined and parallel to the prevailing wind; (see Wang *et al*., 2011, fig. 1). The morphology, sedimentology, classification, and distribution of yardangs in this area have been studied elsewhere (Dong *et al*., 2012; Qu *et al*., 2014). The Gravel Bodies described here differ from the nearby yardangs in the Achike Valley, as they are covered by gravel (Fig. 3a). Our field surveys undertaken between July 2007 to June 2014, together with the works of E *et al*. (2008) and Tang *et al*. (2011), clearly

Figure 2. The so-called 'gravel bodies' in the Kumtagh Desert can be classified into two types according to their plan-view shapes. (a) Elongated 'gravel body'; (b) Subround 'gravel body'. This figure is available in colour online at wileyonlinelibrary.com/journal/gj

DOI: 10.1002/gj

Figure 3. Close-up of the 'gravel body'. (a) All gravel bodies are covered by sediments sizing from coarse sand to boulders. The biggest boulder exceeds 1.0 m in diameter. (b) There are layers of sand, calcrete, gypsum, halite, and/or solidified mud beneath the surficial gravel layer. This figure is available in colour online at wileyonlinelibrary.com/journal/gj

show that (1) the so-called 'gravel body' is not composed of gravel entirely. The thickness of the surface gravel layer varies between 0.20 m to 1.20 m. The biggest *in situ* gravel or boulder observed exceeds 1.0 m in diameter. There are layers of sand, calcrete, gypsum, halite, and/or solidified mud beneath the gravel layer. The sand layers in a subround 'gravel body' are shown in Figure 3b. (2) Imbrication has been frequently observed in the gravel layer. Although the directions of long axes of gravels are generally identical for an individual gravel body, the orientation of gravel bodies is irregular. In the 114 measured gravel bodies, the imbrication trends of NbE, NbW, and E-W are 52.6%, 43.9%, and 3.5% in percentage terms, respectively (E *et al*., 2008). Although weathering process could generate local gravel deposits in deserts (Rajaguru *et al*., 1996), the characteristics depicted above support an extraneous origin. There are four major kinds of continental depositional systems (Boggs, 2005). The sediment size excludes gravels and boulders from lacustrine and aeolian deposits. The Kumtagh Desert at relatively low elevations was not an accumulation area of glacial sediments. By this simple process of elimination, a fluvial origin is most likely. Both debris-flow and stream-flow deposits may contain gravels and boulders. The debris-flow deposits occasionally found on the northern slope of the Altyn Mountains are characterized by the chaotic mosaic of various sized sediments, and commonly associated with landslide deposits. A debris-flow origin to the gravel bodies once was suspected, until likely palaeochannels were interpreted (Dong *et al*., 2010). The elongated gravel bodies share some morphologic similarity with straight river channels. The large gravels and boulders with preferred orientations indicate that the gravel bodies were most likely deposited from stream-flow.

Following Oviatt *et al*. (2003), here we use the term 'gravel channel' rather than gravel body to describe this type of landform in the Kumtagh Desert. The largest drainage area on the northern slope of the Altyn Mountains is that of the Suosuogou River (Lu, 2012). At present, it is a dry valley and only receives fluvial discharge during flash flood events. Figure 4 gives the spatial distribution of gravel channels in the lower reaches of the Suosuogou River. In the northeastern and central parts of the area, gravel channels are sparse and absent, and only the subround type occurs. In the southwestern part of the study area, both types are found and widely distributed. We interpret the distribution of gravel channels as comprising distributaries of an alluvial fan delta. A drilling core revealed that the Altyn-Beishan intermontane basin was occupied by a large body of water in the late Middle Pleistocene (Wang and Zhao, 2001). At that time, the present day Achike Valley and the Xihu playa lake area resided in the Lop Nor palaeolake with a lake level exceeding 840 m in elevation (Lu, 2012). The *in situ* remaining lacustrine deposits protected by gravels or boulders imply that the lake level reached a maximum elevation of at least 900 m. This indicates that some gravel channels with a present-day elevation range of between 830–965 m (shown in Fig. 4) were subaqueous, or that the lake levels fluctuated extensively. It is currently difficult to accurately model the palaeoshoreline distribution as subsequent to its desiccation the area has been severely eroded and deeply weathered. Additional field work is required to detail the geometry and extent of the alluvial fan.

3.2. Physical modelling

To estimate wind erosion rate, the age T and the position H of the former terrestrial ground surface must be determined. As for T, the aeolian sands at the base of the gravel layer were used for OSL dating of the inverted relief landforms. The chronological samples were measured in the OSL laboratory of Nanjing University (Lu, 2012). H comprises two components: the present height h of the inverted relief feature and the eroded height H_0 above the remnant gravel channel top. The latter component is difficult to ascertain due to subsequent wind erosion. Fortunately, some methods of reconstructing channel geometry and palaeohydrology associated with past flood events for arid river systems have been developed (Baker, 2008; Goudie, 2013). Palaeohydrological

DOI: 10.1002/gj

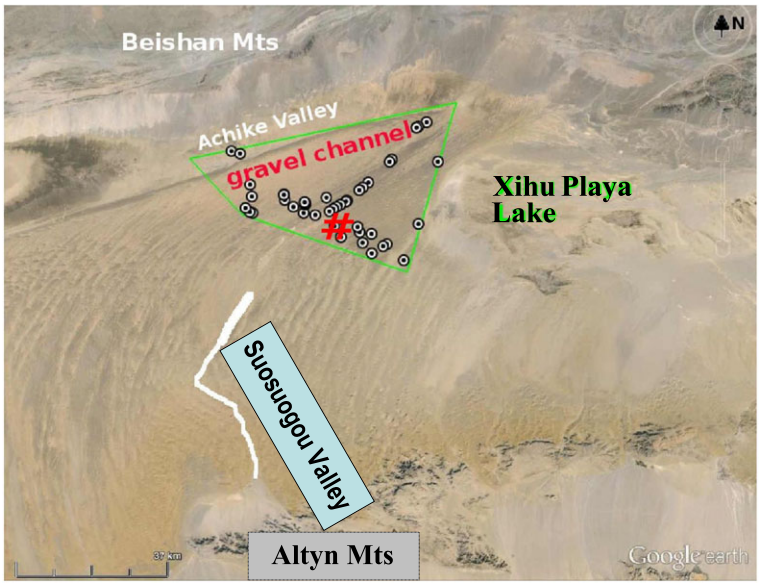

Figure 4. The spatial distribution of gravel channels in the lower reaches of the Suosuogou Valley. The valley course is indicated by the white curve. The symbol '⊙' denotes an individual gravel channel, and their distribution area is restricted by the green lines. The symbol '#' marks the OSL sampling site. This figure is available in colour online at wileyonlinelibrary.com/journal/gj

parameters can be estimated by using the empirical or theoretical relations between boulder size and flow velocity (Kehew *et al*., 2010). A valuable tool for understanding past floods is the high-resolution computational fluid dynamics simulation underpinned by classical mechanics theory (Denlinger and O'Connell, 2010). Some assumptions must be made for reconstructing the palaeohydrology of the gravel channels. The Suosuogou Valley (Fig. 4) has meandering channel components, but overall it comprises a linear geometry except at one inflection point. Hereinafter, we assume a straight channel with a constant width and slope. The coarse sediments including gravels and boulders begin to deposit when a flood exits from mountain valleys, and when the transportation capability of the stream is reduced by increasing flow width. The alluvial depositions in the gravel channels would represent the cumulative result of a number of different flood events. Noting that extreme floods are very rare and an alluvial river often changes its course in the sediment deposition zone, we assume that the surface gravel layer of the inverted relief features was deposited by a single flood event, and subsequent discharge events in the former channels were incapable of moving large boulders. We also assume that the present-day surficial depositions comprise the basal gravel layer of the pre-existing fluvial channel. Under these assumptions, a conservative, minimum approximation of H_0 may be calculated, being based upon the maximal flow depth reconstructed from boulder size data.

In the case where almost all the alluvial sediments deposited in the former channel have been removed by wind, the maximum thickness of the palaeochannel may be roughly estimated, by making assumptions of the sediment transportation capacity of the reconstructed flood. The sum of this palaeochannel thickness and the maximal flow depth can be regarded as the upper limit of H_0.

3.2.1. *Palaeoflood reconstruction*

The mean flow velocity of the flood U can be expressed by the Manning (or Gauckler–Manning–Strickler) formula (Gioia and Bombardelli, 2002),

$$U = \frac{k}{n} R^{\frac{2}{3}} \tan^{\frac{1}{2}}\theta \tag{1}$$

where k, n, R, and θ are the conversion factor, Manning coefficient, hydraulic radius, and the slope angle of channel bed, respectively.

When the width w of a rectangular channel is much larger than the flow depth D, the hydraulic radius R is reduced to,

$$R = \frac{wD}{w + 2D} \approx D \tag{2}$$

The particle size of sediments often reflects hydrodynamic conditions. Boulders in the gravel channels are interpreted to have been mainly transported by flash floods from the Altyn Mountains. Flow velocity is a function of boulder size (Costa, 1983; Benner *et al*., 2010; Stokes *et al*., 2012). For a cuboid boulder with dimensions of a, b, and c at the motion instant, the resulting moment about the point of 'O' must be zero, as shown in Figure 5. Comparing with drag F_d and gravity mg, the lift force F_l is negligible. The action point of supporting force N is 'O'. Thus, the moment balance equation is

DOI: 10.1002/gj

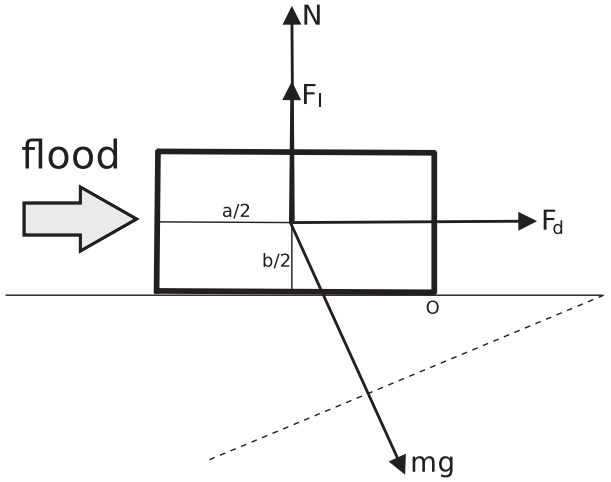

Figure 5. Forces on a boulder. The resulting moment about the point of '*O*' must be zero at the motion instant.

$$F_d b + mgb\ \sin\theta\ =\ mga\ \cos\theta \tag{3}$$

in which g is the gravity acceleration.

The drag force F_d and mass m can be written as,

$$F_d = \frac{1}{2}\rho_w C_d bcU^2 \tag{4}$$

and

$$m = \rho_s abc \tag{5}$$

where ρ_w and ρ_s are the density of water and the boulder. The drag coefficient C_d depends on the boulder shape and flow regime (Benner *et al*., 2010). For simplicity, it is treated here as a constant because the Reynolds number is large enough in a flash flood.

Combining equations (1) to (5), we have

$$D \approx \left(\frac{n}{k}\right)^{\frac{3}{2}}\left[\frac{2}{C_d}\frac{\rho_s}{\rho_w} ga\ \cos\theta\left(\frac{a}{b}\cot\theta - 1\right)\right]^{\frac{3}{4}} \tag{6}$$

3.2.2. Maximum thickness of the palaeochannel bed

Assuming the suspended materials being transported by the flood were uniformly deposited in the flow direction, the mass conservation equation becomes

$$\rho_s CDUt = \rho_b D_0 L \tag{7}$$

where C is the mean sediment concentration by volume, t is the flood duration, ρ_b is the bulk density of the channel bed, D_0 is the channel bed thickness, and L is the channel length in the deposition zone.

There are numerous formulae for estimating the transport rate of bed and suspended load (Qian and Wan, 2003; Chanson, 2004). For desert flash-floods, some empirical relations fitted for the field data of certain rivers have been established, (see Billi, 2011 and references therein). Sediment concentration (or transport rate) often changes with flow velocity, discharge, shear stress, and grain-size. When the maximum sediment concentration $C = C_{max}$ is kept during the flood, we get the maximum thickness of the palaeochannel from equation 7,

$$D0 = \frac{\rho_s C_{max} Ut}{\rho_b L} \tag{8}$$

3.2.3. Wind erosion rate

Given the age T and the present height h of the gravel channel, the wind erosion rate η can be estimated by,

$$\eta = \frac{H}{T} = \frac{h + Ho}{T} \tag{9}$$

The energy conditions of water and wind deposition vary greatly. Two extreme scenarios are considered. We assume the minimum eroded height H_0 is equal to the maximum flow depth D, when the channel bed can effectively resist the subsequent wind erosion. In this case, the minimum wind erosion rate can be expressed by,

$$\eta_{\min} = \frac{h + D}{T} \tag{10}$$

The dried channel bed composed of loose sediments sizing from clay to sand may be easily eroded by wind. In this case, the main body of the former channel bed has been eroded, with the thin veneer of preserved gravels and boulders representing the basal layer of the former alluvial channel. If this interpretation is correct, the inferred maximum wind erosion rate can be written as,

$$\eta_{\max} = \frac{h + D + D_0}{T} \tag{11}$$

4. RESULTS

The parameters in the estimation of wind erosion rate are listed in Table 1. The geometrical parameters a and b of larger boulders, the mean slope angle θ of the Suosuogou Valley, and the length L of the palaeochannel bed were obtained either from our field surveys or from topographic data. The drag coefficient C_d, the conversion factor k, and Manning coefficient n were sourced from Kehew *et al*. (2010) and Benner *et al*. (2010). Noting the floods in this super-arid region of China are reported to last for on average 0.5–6.0 h (Ge, 1983; Chen, 1990), an appropriate

DOI: 10.1002/gj

Table 1. Parameters in the estimation of wind erosion rate

Parameter	Value	Parameter	Value
C_d	1.2	a	0.9 m
k	1.0 $m^{1/3}/s$	b	0.8 m
n	0.05	θ	0.006 m
g	9.81 m/s^2	h	25 m
ρ_s	2.7×10^3 kg/m^3	L	40 km
ρ_w	1.0×10^3 kg/m^3	t	3.0 h
ρ_b	1.5×10^3 kg/m^3	C_{max}	50%

C_d is the drag coefficient. k and n are the conversion factor and Manning coefficient; g is the gravity acceleration. ρ_s, ρ_w, and ρ_b are the densities of boulder, water, and channel bed. a and b are the length and width of the boulder. θ, h, and L are the slope, height, and length of the palaeochannel. t is the duration of the flood. C_{max} is the maximal volume concentration of sediment.

duration t of three hours for the palaeoflood is assumed. The upper limit of volume concentration of sediment transported by flood is 60%, beyond which debris flows occur (Qian and Wan, 2003). In our calculation, $C_{max} = 50\,\%$ is assumed.

4.1. Palaeohydrological parameters and ages

The maximum flow depth D obtained from equation 6 is 6.8 m. The threshold flow velocity driving the motion of sediments is regarded as the depth-averaged flow velocity of the flood. The value of this parameter calculated by equations 3 and 4 is 5.9 m/s. The width of the Suosuogou Valley changes from 10 m to 50 m. Discharge, defined as the product of the flow velocity U, depth D, and width w, is calculated at 1337 m^3/s if a medium width $w = 30$ m is assumed. The empirical Manning formula, widely used in palaeoflood hydrology, is widely accepted to be robust in its assumptions (Gioia and Bombardelli, 2002). Some palaeohydrological reconstructions of floods were listed by Kehew *et al*. (2010). The flood generating the gravel channels in the Kumtagh Desert is comparable with the Elm Greek River flood that occurred in 1972, in Texas, USA. From a physical stand point, the motion of continuous discharge and discrete solid gravel particles can be described by the Navier–Stokes equations and the Euler's laws. Two aspects need to be further considered in modelling arid river discharge using equations 1–6. Firstly, for simplicity the hydraulic radius is replaced with the flow depth. This simplification is suitable for wider channels but might overestimate the flow velocity because the part of $w/(w+2D)$ in equation 2 is increased to 1. Secondly, the model can't provide any information about the flood evolution processes varying with time, because the Manning formula is only suitable to steady flow.

A typical subround-type gravel channel 25 m high at (40°12′51.27″ N, 92°33′24.74″ E) was excavated for determining the age of this unique landform. The aeolian deposits beneath the surface gravel layer with a thickness of 30 cm were an ideal material of the OSL dating method (Aitken, 1998). The age obtained from the quartz grains in the samples is $T = 150.8 \pm 7.5$ ka. The age of the aeolian sands at a depth of 2.9 m from the bank top of the Suosuogou Valley has been calculated at 158.6 ka (Lu, 2012). Although the sediment profile description and chronological approach were not supplied in the latter study, the close agreement between the two values suggests gives confidence in the dating method outcomes. The age of gravel channels 120 km to the west of the Suosuogou Valley to the west has been calculated as 53.1 ± 1.9 ka (Lu, 2012). This data indicate that the inverted relief landforms in the desert were not formed simultaneously, and our study confirms the conclusion of Tang *et al*. (2011) that the gravel channels in the region were developed between 285.9 ± 42.9 ka BP based on the electron spin resonance dating data of three long profiles (two located in the drainage area of the Suosuogou Valley, the other one in the western Desert) with very low temporal resolution.

4.2. Rates of wind erosion

The channel bed thickness forming in three hours is $D_0 = 9.75$m. This value, much larger than the residual thickness of the channel bed in the inverted relief feature, can be used to determine the maximum wind erosion rate. Two extreme values of wind erosion rate calculated by equations 10 and 11 are 0.21 and 0.28 mm/year, respectively. There is no gauged data detailing wind erosion in the study location. Archaeological studies have provided some analogue data on wind erosion. Historiographers were important government officers in historical dynasties in China. The local information about environment, population, products, cities, and wars etc. have been officially recorded by numerous historical sources since the Han dynasty (202–9 BC). By determining the ages of buildings and man-made structures identified in historical records (or the modern dating methods), and assuming that the pre-deflation surface was flat, the wind erosion rate can be estimated. This is a conventional method in aeolian research. The ancient 'Silk Road' from Dunhuang to Loulan (Kroran also) at (40°29′55″ N, 89°55′22″ E) traverses the northern margin of the Kumtagh Desert. The time-averaged wind erosion rate in the now ruined Loulan City since the sixth century has been calculated at 2.44 mm/year (Xia, 2007). There are common remains of human activity in the ancient Gua-Sha oasis, a blowland separated from the Kumtagh Desert by the Xihu playa lake. The current erosive land surface along the Great Wall implies that the wind erosion rate over the past two thousand years is in the range of 0.5–1.5 mm/year. A ruined city at (40°27′12.48″ N, 95°13′33.29″ E) was discovered in 2013. The C-14 age of the cultural layer is 1226–1277 AD, and the mean eroded height is 1.10 m. The local wind

DOI: 10.1002/gj

erosion rate is consequently calculated to be approximately 1.44 mm/year. Comparing the data obtained in the west (Loulan) and east (the ancient Gua-Sha oasis) regions, the wind erosion rate of 0.21–0.28 mm/year in the northern Kumtagh Desert is smaller in magnitude. Surprisingly, the present-day annual wind speeds do not differ significantly between the three areas (Zhang *et al*., 2010; Qu *et al*., 2011). We interpret two dominant reasons for this. Firstly, the widely distributed water-formed deposits can effectively withstand deflation and abrasion. For loose gravelly sediments, the wind speeds capable of entraining them are high. Sand and dust also are difficult to be emitted from the surficial carbonate cement or salt crust of the ground. Secondly, the sediments in this lowland might be supplemented by abrupt floods or persistent rivers after the palaeochannels formed.

5. DISCUSSION

Inverted relief in deserts is a common but not well understood landform. The study of raised channels needs a multidisciplinary approach including geomorphology, geology, hydrology, sedimentology, and geochronology. The present work could provide some useful implications with respect to geomorphology and palaeohydrology.

5.1. Geomorphology

Identification of geomorphic types is the starting point of desert geomorphology studies. The inverted gravel channels we describe here are a unique landform in the Kumtagh Desert. Their formation involved fluvial and aeolian processes in which the fluvial deposits of gravels and boulders effectively withstood subsequent wind erosion, and became the surficial layer of the inverted features. There have been many debates about the relative importance of aeolian and fluvial processes in moulding desert landscapes (Goudie, 2013). Recently, fluvial-aeolian interaction in dryland environments has stimulated much research, e.g. (Al-Masrahy and Pountney, 2015; Yan *et al*., 2015). Our work will be helpful for the quantitative description of the fluvial-aeolian processes responsible for desert landscape development. For the Kumtagh Desert, the dynamic effects of the remnant fluvial deposits on the dune forms, orientations, and spatial distribution remain to be revealed.

The current Martian surface is very similar to that of hyperarid desert on Earth. Our knowledge based on terrestrial analogue studies is potentially significant to explain data returned by probes and to understand the origin of surface features on Mars when a manned mission is lacking (Chapman, 2007). Mars once was subjected to fluvial processes. The outflow channels in the Valles Marineris region were carved by outburst floods probably (Coleman and Baker, 2009). Wind is one of the few known geological processes in action at the Martian surface (Greeley and Iversen, 1985). So the channels in a blowland are more easily to evolve into inverted reliefs naturally. A detailed description and interpretation of Martian inverted channels on a fan are referred to a very recent work of Morgan *et al*. (2014). The arid region in north-western China could offer some ideal sites, e.g. the Qaidam Basin, to perform terrestrial analogue studies. The presented model for the inverted gravel channels in this study is an optional method for estimating the discharge of palaeoflood and the long-term wind erosion rate on Mars.

5.2. Palaeohydrology

Determining accurate thickness of the former channel bed is crucial to wind erosion rate estimation. Palaeochannel morphologic characteristics can be reconstructed empirically (Leeder, 1973; Smith, 1987) or theoretically (Bridge and Diemer, 1983; Zaleha, 2013). A database representing more than 1500 bedrock and Quaternary alluvial channel bodies has been established (Gibling, 2006). Although the dimensions of desert river channels are poorly documented, a likely positive correlation between the width and thickness of fluvial depositions is $w/D = 10$; (see Gibling, 2006, fig. 8 for details). Comparing the value of D or $D + D_0$ that we estimated, the palaeochannel thickness of 3.0 m obtained from this empirical formula is much smaller. For a straight, non-migrating, and incised channel, the relationship $w = 0.01D^{2.9}$ has been fitted (Fielding and Crane, 1987). Inserting $w = 30$ m into this relation, $D = 15.81$ m is obtained. This value is slightly less than the maximum eroded thickness of $D + D_0 = 16.55$ m obtained in our preliminary work. The more specialized physical models, e.g. (Bridge, 1992) and (Tayfur and Singh, 2006), should be introduced to reconstruct the palaeochannel thickness and palaeohydrology. As pointed out by Reid and Frostick (2010), there still is a great need for more detailed information on channel form, flood hydrology, and sediment transport in deserts. Model validation by using data from modern floods represents a challenge as this database is not currently extensive. Moreover, the determination of model parameters will be restricted if the desert surface is being severely reworked by wind. Palaeoflood frequency and extent in this region remain to be investigated in the future.

6. CONCLUSIONS

The study of landforms generated by inverted relief associated with former fluvial palaeochannels in deserts provides a means of assessing the magnitude of subsequent wind

DOI: 10.1002/gj

erosion. A type of inverted relief called the 'Gravel Channel' is identified in the northern Kumtagh Desert. A simple physical model of palaeoflood has been introduced in an attempt to reconstruct the former topography based on mechanical principles and the characteristics of the deposits of the gravel palaeochannel. Pre-channel deposits have been dated using the OSL technique, and subsequently a wind erosion rate has been estimated by using the height of gravel channel, the flow depth, and the eroded thickness of channel bed estimated from palaeoflood modelling. It is shown that the long-term wind erosion rate in the northern Kumtagh Desert is 0.21–0.28 mm/year. Wind erosion occurring in this desert is no more severe than that experienced in adjacent regions.

ACKNOWLEDGEMENTS

Zhen-Ting Wang is grateful to Zhi-Zhu Su, Hua-Yu Lu, and Qi Lu for valuable discussions, to Xiao-Zong Ren, Guo-Qiang Li, and Zhi-Lin Shi *et al.* for their help in the field. The unpublished C-14 age was kindly provided by Guang-Hui Dong. Robert Hillier offered insightful comments and suggestions for improving the quality of this manuscript. This research was supported by NSFC projects (Nos. 11274002, 41272191, and 41571006), the cooperation project of Hebei Academy of Sciences and the Chinese Academy of Sciences (No. 15001019), and State Key Laboratory of Earth Surface Processes and Resource Ecology project (No. 2015-KF-05).

REFERENCES

Aitken, M.J. 1998. *An Introduction to Optical Dating: the Dating of Quaternary Sediments by the using of Photon-stimulated Luminescence*. Oxford University Press: New York; 108–117.

Al-Dousari, A.M., **Al-Elaj, M.**, **Al-Enezi, E.**, **Al-Shareeda, A. 2009**. Origin and characteristics of yardangs in the Um Al-Rimam depressions (N Kuwait). *Geomorphology* **104**, 93–104.

Al-Masrahy, M., **Pountney, N.P. 2015**. A classification scheme for fluvial-aeolian system interaction in desert-margin settings. *Aeolian Research* **17**, 67–88.

Baker, V.R. 2008. Palaeoflood hydrology: origin, progress, prospects. *Geomorphology* **101**, 1–13.

Benner, R., **Browne, T.**, **Bruckner, H.**, **Kelletat, D.**, **Scheers, A. 2010**. Boulder transport by waves: progress in physical modelling. *Zeitschrift für Geomorphologie* **54**(suppl), 127–146.

Billi, P. 2011. Flash flood sediment transport in a steep sand-bed ephemeral stream. *International Journal of Sediment Research* **26**, 193–209.

Boggs, S. Jr. 2005. *Principles of Sedimentology and Stratigraphy*. Pearson Prentice Hall: New Jersey; 241–288.

Bridge, J.S. 1992. A revised model for water flow, sediment transport, bed topography and grain size sorting in natural river bends. *Water Resources Research* **28**, 999–1013.

Bridge, J.S., **Diemer, J.A. 1983**. Quantitative interpretation of an evolving ancient river system. *Sedimentology* **30**, 599–623.

Bristow, C.S., **Drake, N.**, **Armitage, S. 2009**. Deflation in the dustiest place on Earth: the Bodélé Depression, Chad. *Geomorphology* **105**, 50–58.

Brookes, I.A. 2003. Palaeofluvial estimates from exhumed meander scrolls, Taref Formation (Turonian), Dakhla Region, Western Desert, Egypt. *Cretaceous Research* **24**, 97–104.

Chanson, H. 2004. *Hydraulics of Open Channel Flow*. Butterworth-Heinemann: Amsterdan; 143–238.

Chapman, M.G. (Ed). **2007**. *The Geology of Mars: Evidence from Earth-Based Analogs*. Cambridge University Press: Cambridge; 1–460.

Chen, Y.N. 1990. The study on the types and characteristics of hazardous floods in the Tarim Basin's edge. *Journal of Arid Research* **7**, 45–52 [in Chinese with English abstract].

Chen, K., **Bowler, J.M. 1986**. Late Pleistocene evolution of salt lakes in the Qaidam basin, Qinghai province, China. *Palaeogeography, Palaeoclimatology, Palaeoecology* **54**, 87–104.

Clarke, M.L., **Wintle, A.G.**, **Lancaster, N. 1996**. Infra-red stimulated luminescence dating of sands from the Cronese Basins, Mojave Desert. *Geomorphology* **17**, 199–205.

Coleman, N.M., **Baker, V.R. 2009**. Surface morphology and origin of outflow channels in the Valles Marineris region. In: *Megaflooding on Earth and Mars*, Burr, D.M., Carling, P.A., Baker, V.R. (eds). Cambridge University Press: Cambridge; 172–193.

Costa, J.E. 1983. Palaeohydraulic reconstruction of ash flood peaks from boulder deposits in the Colorado Front Range. *Geological Society of America Bulletin* **94**, 986–1004.

Denlinger, R.P., **O'Connell, D.R.H. 2010**. Simulations of cataclysmic outburst floods from Pleistocene Glacial Lake Missoula. *GSA Bulletin* **122**, 678–689.

Dong, Z. 2009. The identification of feathery dunes. *Science & Technology Review* **27**, 69–75 [in Chinese with English abstract].

Dong, Z., **Lv, P. 2014**. Recent advances in research on the aeolian geomorphology of China's Kumtagh Sand Sea. *Advances in Geosciences* **37**, 41–46.

Dong, Z., **Qu, J. 2009**. *Introduction to Geomorphic Map of the Kumtagh Desert*. Science Press: Beijing; 37–40 [in Chinese with English abstract].

Dong, Z., **Qu, J.**, **Wang, X.**, **Qian, G.**, **Luo, W.**, **Wei, Z. 2008**. Pseudo-feathery dunes in the Kumtagh Desert. *Geomorphology* **100**, 328–334.

Dong, Z., **Qian, G.**, **Yan, P.**, **Su, Z. 2010**. Gravel bodies in the Kumtagh Desert and their geomorphological implications. *Environmental Earth Sciences* **59**, 1771–1779.

Dong, Z., **Su, Z.**, **Qian, G.**, **Luo, W.**, **Zhang, Z.**, **Wu, J. 2011**. *Aeolian Geomorphology of the Kumtagh Desert*. Science Press: Beijing; 231–235 [in Chinese with English abstract].

Dong, Z., **Lv, P.**, **Lu, J.**, **Qian, G.**, **Zhang, Z.**, **Luo, W. 2012**. Geomorphology and origin of Yardangs in the Kumtagh Desert, Northwest China. *Geomorphology* **139–140**, 145–154.

E, Y., **Su, Z.**, **Wang, J.**, **Zhai, X.**, **Liu, H. 2006**. Outcome and scientific significance of integrated investigation in Kumtag Desert. *Journal of Desert Research* **26**, 693–697 [in Chinese with English abstract].

E, Y., **Wang, J.**, **Yan, P.**, **Gao, S.**, **Wang, X.**, **Su, Z.**, **Liao, K.**, **Liu, H.**, **Ding, F. 2008**. Evolution of palaeo-drainage system and its relationship with the formation of desert landform in the Kumtag Desert. *Acta Geographica Sinica* **63**, 725–734 [in Chinese with English abstract].

Fielding, C.R., **Crane, R.C. 1987**. An application of statistical modelling to the prediction of hydrocarbon recovery factors in fluvial reservoir sequences. *The Society of Economic Paleontologists and Mineralogists* Special Publication **39**, 321–327.

Fryberger, S.G. 1979. Dune forms and wind regime. In: *A Study of Global Sand Seas*, McKee, E.D. (ed). *Geological Survey Professional Paper* 1052, U.S. Government Printing Office: Washington; 137–170.

Ge, Q.F. 1983. Super-arid regions in China and hazardous floods. *Meteorological Monthly* **22**, 34–35 [in Chinese with English abstract].

Gibling, M.R. 2006. Width and thickness of fluvial channel bodies and valley fills in the geological record: a literature compilation and classification. *Journal of Sedimentary Research* **76**, 731–770.

Gioia, G., **Bombardelli, F.A. 2002**. Scaling and similarity in rough channel flows. *Physical Review Letters* **88**, 014501.

Goossens, D., **Offer, Z.**, **London, G. 2000**. Wind tunnel and field calibration of five aeolian sand traps. *Geomorphology* **35**, 233–252.

Goudie, A.S. 2013. *Arid and Semi-Arid Geomorphology*. Cambridge University Press: Cambridge; 114–159, 204–245.

Greeley, R.G., Iversen, J.D. 1985. *Wind as a Geological Process on Earth, Mars, Venus and Titan*. Cambridge University Press: Cambridge; 1–32.

Hagen, L.J. 1991. A wind erosion prediction system to meet user needs. *Journal of Soil and Water Conservation* **46**, 106–111.

He, Q., Yang, X., Huo, W., Wang, S., Shang, K., Liu, H.Y. 2009. Characteristics of sand granularity from Kumtag Desert and its environmental significance. *Journal of Desert Research* **29**, 18–22 [in Chinese with English abstract].

Horner, N.G. 1932. Lop Nor: topographical and geological summary. *Geografiska Annaler* **14**, 297–321.

Kang, Y.Z., Chen, S.H., Zhang, Y., Wang, S.H., Shang, K.Z., Cheng, Y.F. 2015. Precipitation during 2008–2013 in the Kumtagh desert and Altun mountains. *Journal of Desert Research* **35**, 203–210 [in Chinese with English abstract].

Kehew, A.E., Milewski, A., Soliman, F. 2010. Reconstructing an extreme flood from boulder transport and rainfall runoff modelling: Wadi Isla, South Sinai, Egypt. *Global and Planetary Change* **70**, 64–75.

Lai, Z.P., Mischke, S., Medsen, D. 2014. Palaeoenvironmental implications of new OSL dates on the formation of the 'Shell Bar' in the Qaidam Basin, northeastern Qinghai-Tibetan Plateau. *Journal of Palaeolimnology* **51**, 197–210.

Laity, J.E. 2009. Landforms, landscapes, and processes of aeolian erosion. In: *Geomorphology of Desert Environments*, Parsons, A.J., Abrahams, A. D. (eds). Springer: Amsterdan; 597–627.

Laity, J.E. 2011. Wind erosion in drylands. In: *Arid Zone Geomorphology*, Thomas, D.S.G. (ed). Wiley-Blackwell: Oxford; 539–568.

Lal, D. 1991. Cosmic ray labeling of erosion surfaces: in situ nuclide production rates and erosion models. *Earth and Planetary Science Letters* **104**, 424–439.

Leeder, M.R. 1973. Fluviatile fining-upwards cycles and the magnitude of palaeo-channels. *Geological Magazine* **110**, 265–276.

Lu, Q. (Ed). **2012**. *A Study of the Kumtag Desert*. Science Press: Beijing; 45–48, 129–133, 233–241, 261–269 [in Chinese with English abstract].

Maizels, J.K. 1987. Plio-Pleistocene raised channel systems of the western Sharqiya (Wahiba), Oman. *Geological Society (Special Publications)* **35**, 31–50.

Maizels, J.K. 1990. Raised channel systems as indicators of palaeohydrologic change: a case study from Oman. *Palaeogeography, Palaeoclimatology, Palaeoecology* **76**, 241–277.

Malin, M.C., Edgett, K.S. 2003. Evidence for persistent flow and aqueous sedimentation on early Mars. *Science* **203**, 1931–1934.

Morgan, A.M., Howard, A.D., Hobley, D.E.J., Moore, J.M., Dietrich, W.E., Williams, R.M.E., Burr, D.M., Grant, J.A., Wilson, S.A., Matsubara, Y. 2014. Sedimentology and climatic environment of alluvial fans in the martian Saheki crater and a comparison with terrestrial fans in the Atacama Desert. *Icarus* **229**, 135–156.

Oviatt, C.G., Madsen, D.B., Schmitt, D.N. 2003. Late Pleistocene and early Holocene rivers and wetlands in the Bonneville basin of western North America. *Quaternary Research* **60**, 200–210.

Pain, C.F., Ollier, C.D. 1995. Inversion of relief-a component of landscape evolution. *Geomorphology* **12**, 151–165.

Pain, C.F., Clarke, J.D.A., Thomas, M. 2007. Inversion of relief on Mars. *Icarus* **190**, 478–491.

Pelt, R.S.V., Peters, B., Visser, S. 2009. Laboratory wind tunnel testing of three commonly used saltation impact sensors. *Aeolian Research* **1**, 55–62.

Qian, N., Wan, Z.H. 2003. *Mechanics of Sediment Transport*. Science Press: Beijing; 275–393, 430-449[in Chinese].

Qian, G., Dong, Z., Zhang, Z., Luo, W., Lu, J., Yang, Z. 2015. Morphological and sedimentary features of oblique zibars in the Kumtagh Desert of Northwestern China. *Geomorphology* **228**, 714–722.

Qu, J.J., Liao, K.T., Zu, R.P., Xia, X.C., Jing, Z.F., Dong, Z.B., Zhang, K.C., Yang, G.S., Wang, X.M., Dong, G.T. 2007. Study on formation mechanism of feather-shaped sand ridge in Kumtag Desert. *Journal of Desert Research* **27**, 349–354 [in Chinese with English abstract].

Qu, J.J., Liao, K.T., Dong, G.R., Niu, Q.H., Jing, Z.F., Han, Q.J. 2011. Feathered sand ridges in the Kumtagh Desert and their position in the classification system. *Science China Earth Sciences* **54**, 1215–1225.

Qu, J.J., Niu, Q.H., Gao, D.X. 2014. *Formation and Development Processes Pattern of Dunhuang Yardang Landforms*. Geological Publishing House: Beijng; 1–166.

Rajaguru, S.N., Mishra, S., Ghate, S. 1996. A re-interpretation of gravel spreads in the Jaisalmer region, Thar Desert, India. *Journal of Arid Environments* **32**, 53–58.

Reid, I., Frostick, L.E. 2010. Channel form, flows and sediments of endogenous ephemeral rivers in desert. In: *Arid Zone Geomorphology*, Thomas, D.S.G. (ed). Wiley-Blackwell: Oxford; 301–332.

Rohrmann, A., Heermance, R., Kapp, P., Cai, F. 2013. Wind as the primary driver of erosion in the Qaidam Basin, China. *Earth and Planetary Science Letters* **374**, 1–10.

Ruszkiczay-Rudiger, Z., Braucher, R., Csillag, G., Fodor, L.I., Dunai, T.J., Bada, G., Bourles, D., Muller, P. 2011. Dating Pleistocene aeolian landforms in Hungary, Central Europe, using in situ produced cosmogenic ^{10}Be. *Quaternary Geochronology* **6**, 515–529.

Shao, Y., Raupach, M., Short, D. 1994. Preliminary assessment of wind erosion patterns in the Murray-Darling Basin. *Australian Journal of Soil and Water Conservation* **2**, 181–204.

de Silva, S.L., Bailey, J.E., Mandt, K.E., Viramonte, J.M. 2010. Yardangs in terrestrial ignimbrites: synergistic remote and field observations on Earth with applications to Mars. *Planetary and Space Science* **58**, 459–471.

Smith, R.M.H. 1987. Morphology and depositional history of exhumed Permian point bars in southwestern Karoo, South Africa. *Journal of Sedimentary Petrology* **57**, 19–29.

Stokes, M., Grifths, J.S., Mather, A. 2012. Palaeoflood estimates of Pleistocene coarse grained river terrace landforms (Rio Almanzora, SE Spain). *Geomorphology* **149–150**, 11–26.

Tang, J.N., Su, Z.Z., Ding, F., Zhu, S.J., E, Y.H., Zhai, X.W., Yi, Z.Y., Liu, H.J., Zhang, J.C., Li, F.M. 2011. The formation age and evolution of Kumtagh Desert. *Journal of Arid Land* **3**, 114–122.

Tayfur, G., Singh, V.P. 2006. Kinematic wave model of bed profiles in alluvial channels. *Water Resources Research* **42**, W06414.

Walker, M. 2005. *Quaternary Dating Methods*. John Wiley & Sons Ltd.: Chichester; 1–286.

Wang, T. (Ed). **2011**. *Desert and Aeolian Desertification in China*. Science Press: Beijing; 110–149, 598–610.

Wang, Y., Zhao, Z.H. 2001. Quaternary palaeogeography of Aqick depression, Eastern Lop Nur, XinJiang. *Journal of Palaeogeography* **3**, 23–28 [in Chinese].

Wang, Z.-T., Sun, Q.-F., Ren, X.-Z., Wang, T., Chen, F.-H. 2009. Pseudo-feathery dunes in the Kumtagh desert reclassified as linear dunes and zibars. *Aeolian Research* **1**, 87–89.

Wang, Z.-T., Wang, H.-T., Niu, Q.-H., Dong, Z.-B., Wang, T. 2011. Abrasion of Yardangs. *Physical Review E* **84**, 031304.

Williams, R.M.E. 2007. Global spatial distribution of raised curvilinear features on Mars. *Lunar and Planetary Science* **XXXVIII**, 1821.

Woodruff, N.P., Siddoway, F.H. 1965. A wind erosion equation. *Proceeding Soil Science Society of America* **29**, 602–608.

Xia, X. (Ed). **2007**. *Lop Nur in China*. Science Press: Beijing; 55–91 [in Chinese].

Xu, Z.W., Lu, H.Y., Zhao, C.F., Wang, X.Y., Su, Z.Z., Wang, Z.T., Liu, H.Y., Wang, L.X., Lu, Q. 2011. Composition, origin and weathering process of surface sediment in Kumtagh Desert, Northwest China. *Journal of Geographical Sciences* **21**, 1062–1076.

Yan, P., Li, X.M., Ma, Y.F., Wu, W., Qian, Y. 2015. Morphological characteristic of interactions between deserts and rivers in northern China. *Aeolian Research*, doi:10.1016/j.aeolia.2015.01.005 [in press].

Zaleha, M.J. 2013. Paleochannel hydraulics, geometries, and associated alluvial architecture of Early Cretaceous rivers, Sevier Foreland Basin, Wyoming, USA. *Cretaceous Research* **45**, 321–341.

Zhang, H., Wang, Q., Peng, J., Chen, G. 2008. Ostracod assemblages and their palaeoenvironmental significance from Shell Bar section of palaeolake Qarhan, Qaidam Basin. *Quaternary Science* **28**, 103–111 [in Chinese with English abstract].

Zhang, Z., Dong, Z., Zhao, A., Qian, G. 2010. Characteristic of blown sand activity in the Kumtagh Desert. *Arid Land Geography* **33**, 939–936 [in Chinese with English abstract].